Journal of Geomine (2024), 2(1), 43-49
DOI: 10.22077/jgm.2025.8363.1039

Investigation of the Effect of Rock Characteristics on Crack Initiation and Crack Damage Stress Levels in Intact Rock Direct Shear Tests

Mohsen Alidaryan[1], Mohammad Hossein Khosravi[2], Mojtaba Bahaaddini[1], Morteza Ahmadi[3], Erfan Amini[1]

Recived: 2024 Nov. 02, Revised: 2025 Jan. 19, Online Published: 2025 Feb. 02

ABSTRACT

The increasing prevalence of deep mining and civil excavations has highlighted the significance of understanding and analyzing the failure of intact rock. Two critical stress levels in this context are the crack initiation stress and the crack damage stress, both of which are vital for understanding rock behavior during failure. Although numerous laboratory studies have been conducted on the compressive failure of intact rock, there are very few studies that analyze these two stress levels during the shear failure of intact rock. Previously, limited studies were conducted on granite rock. However, in this study, a synthetic rock sample with a much lower uniaxial compressive and tenslie strength than granite was created in the laboratory to examine the impact of other rock characteristics on the levels of crack initiation and crack damage stress in direct shear tests of intact rock. Both numerical modeling using discrete elements and physical modeling of direct shear tests on intact rock, along with acoustic emission analysis, were employed in this study. It was determined that for the rock sample of this study, the crack initiation and crack damage stress levels occurred at approximately 69% and 96% of the peak shear strength, respectively. This result supports previous investigations by showing that these stress levels occur in closer levels to the peak in direct shear tests rather than the uniaxial compressive tests. Moreover, it is showed that these shear stress levels is affected by rock characteristics like porosity, tensile strength, as same as the compressive stress conditions.

KEYWORDS

Crack Initiation Stress, Crack Damage Stress, Direct Shear Test, Peak Shear Strength

I. INTRODUCTION

Before 2000, underground mining depths usually did not exceed 500 meters. Since then, there has been dramatically growth in the depth of new mining projects. For example, in Canada and South Africa, mining depths have surpassed 2,500 meters to access deeper resources. Additionally, in parts of Europe, railway tunnel construction has occurred in locations with over 2,000 meters of overburden (Rahjoo, 2019).

The considerable increase in the depth of underground projects warns us that our previous knowledge on various aspects such as brittle rock failure, instability mechanisms, and common simplifications in engineering design may no longer be precise (Rahjoo, 2019). As the depth of mining and underground excavations increases, intact rock becomes more involved in the failure process. Rock failure at great depths sometimes occurs explosively and rapidly, posing vital life risk to personnel and equipment. It is clear that, understanding of the failure of intact rock has become more critical nowadays. Several studies have been conducted on the brittle failure of intact rock, investigating the failure characteristics and deformation of intact rock (Bieniawski, 1967; Lajtai & Lajtai, 1974; Martin & Chandler, 1994). Results from these studies show that intact rock failure involves three stress levels: crack initiation, crack damage, and peak stress. Crack initiation stress is the point where stable crack growth begins and would stop if loading is halted. Crack damage stress is a level of stress where unstable crack growth starts rapidly and continues even if loading stops. It worth mentioning that the crack initiation does not reduce the strength of rock while the crack damage stress causes significant structural damage and is followed by final failure. Moreover, due to the importance of these two stress levels in understanding intact rock failure, several studies have been conducted in recent decades to study these stress levels. In a standard uniaxial compressive strength test, it is expected that crack initiation stress occurs at about 40% and crack damage stress at about 80% of the peak compressive strength, dividing the stress-strain curve of brittle intact rock failure into five distinct parts (Martin & Chandler, 1994). Fig. 1 shows an example of the stress-strain curve in an axial compression test.

[1]School of Mining Engineering, College of Engineering, University of Tehran, Tehran, Iran, [2]Department of Mining Engineering, Faculty of Engineering, University of Birjand, Birjand, Iran, [3] Department of Mining Engineering, Faculty of Mining and material Engineering, Tarbiat Modares University, Tehran, Iran

✉ M.H.Khosravi: mh.khosravi@birjand.ac.ir; M. Bahaaddini: m.bahaaddini@ut.ac.ir

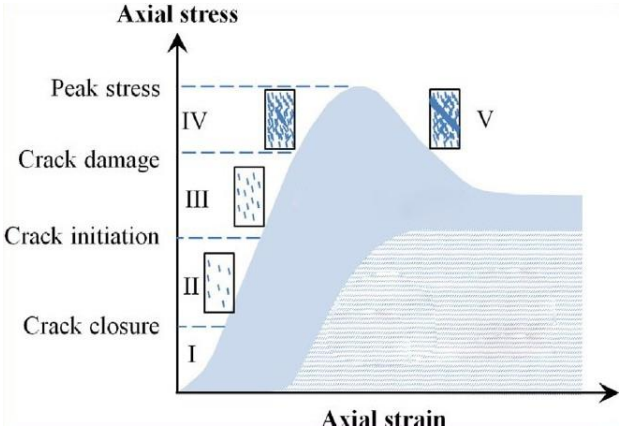

Fig. 1. Brittle failure in intact rocks under compression with illustration of crack initiation and crack damage stress levels (Rafiei Renani & Martin, 2018).

As illustrated in Fig. 1, the failure of intact rock can be divided into five different regions. The initial part of the curve pertains to the closure of pre-existing micro-cracks within the sample. This part may or may not be present, depending on the density and geometry of these initial cracks. Once the micro-cracks close, the rock is considered a linear, homogeneous, and elastic material. At around 40% of the compressive strength, rock dilation and the growth of cracks parallel to the loading direction typically occur. Since the continuation of this crack growth is contingent on ongoing loading, this stress level is termed crack growth stress or crack initiation stress, marking the beginning of the third section (Martin and Chandler, 1994). Previous studies indicate that stresses close to crack initiation stress do not reduce rock strength (Martin and Chandler, 1994). At approximately 80% of uniaxial compressive strength, where axial strain deviates from linearity, the fourth section begins. At this stress level, cracks grow unstably, crack density increases approximately sevenfold, and significant structural changes occur within the sample. This stress level is called crack damage stress (Martin and Chandler, 1994). The onset of the fifth region, or the post-peak region, coincides with uniaxial compressive strength. Martin and Chandler's (1994) study shows that peak stress depends on loading conditions and sample size, while crack initiation stress (σ_{ci}) and crack damage stress (σ_{cd}) do not exhibit this characteristic. As illustrated in Fig. 2, increasing the diameter of Lac du Bonnet granite samples results in minimal changes in crack initiation and crack damage stresses, In contrast, uniaxial compressive strength shows a decreasing trend.

Except for the largest tested sample dimensions, with increasing sample size, peak strength moves toward crack damage stress (Martin and Chandler, 1994). This study has shown that in a uniaxial compression test with monotonic loading, the actual peak strength of the rock equals the crack damage stress. This stress level is also a significant concept in concrete industries and has historically been used to calculate long-term concrete strength. Despite extensive research on crack initiation and crack damage stress levels over the past decades, most studies have been based on compression test analysis. For example, Mutaz et al. (2021) examined over 3,000 existing compression test data on various sedimentary, igneous, and metamorphic rocks. They concluded that there is a linear relationship between crack initiation stress, porosity, and tensile strength of the rock. The study indicates that crack initiation stress increases with tensile strength and decreases with porosity.

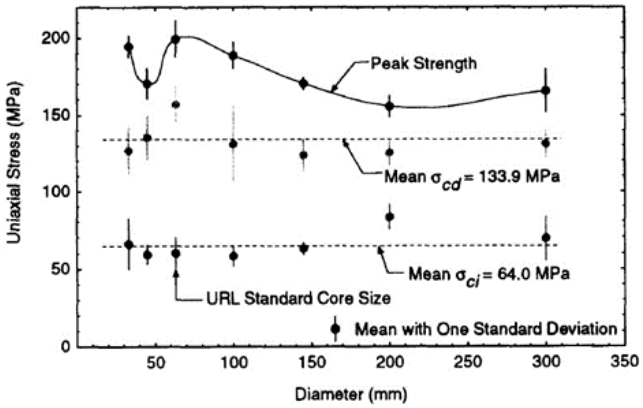

Fig. 2. Effect of sample diameter on peak strength, crack initiation stress, and crack damage stress in Lac du Bonnet granite (Martin and Chandler, 1994).

Peng et al. (2018), after analyzing about 900 previous compression test data, stated that the rock type does not affect the ratio of crack initiation stress and damage stress to peak stress. Their findings also show that in igneous rocks, as grain size increases, both stress levels decrease. Amann et al. (2014) studied the failure of heterogeneous rock-containing stronger veins than the matrix. They concluded that the ratio of crack initiation stress to peak compressive strength could be misleading in identifying the failure process of such rocks. The peak strength depends on the density of hard veins, while cracks initiate in the matrix at lower stresses, even when the peak strength is far from reached.

Li et al. (2020) examined crack initiation and damage stress in shale with seven different bedding orientations under compression. Their results show that crack initiation stress is independent of bedding orientation, but crack damage stress is highly dependent on the rock's anisotropic properties. Various methods have been used to analyze crack initiation and damage stress in axial compression tests, including energy dissipation theory (Ning et al., 2018), moving point regression technique on stress-strain data with acoustic emission analysis (Eberhardt et al., 1998), and wave transmission method (Zhang et al., 2020). However, studies on shear failure of intact rock are very limited and rarely were done. Shang et al. (2021) studied acoustic emissions of a specific granite type and found that the ratio of crack initiation stress and crack damage stress to peak shear strength is 80% and 88%, respectively. Recently,

Alidaryan et al., 2023 investigated the intact rock direct shear test (DST) numerically with a distinct element method through the PFC program. The tested materials was synthetic made of Sulfaset and results showed that for brittle failure type, crack initiation shear stress and crack damage shear stress levels occur in 91% and 95%, respectively. These ratios differ from those reported in compression tests and were examined under brittle failure conditions. It seems that this difference is primarily because of the laboratory test types. This research aims to examine whether rock characteristics influence these stress levels in direct shear tests of intact rock to fill the gap of investigations in DSTs. To this end, both distinct element modeling and physical modeling, along with acoustic emission analyses, have been conducted.

This study utilized numerical and physical modelling of direct shear tests. Over the past decades, advancements in discrete element modeling, mainly using PFC software, have enabled the study of various mechanical parameters of rock, including the number of cracks formed under different test conditions and loadings (Bahaaddini et al., 2021; Bello Garcés, 2018; D O Potyondy, 2018; Potyondy and Cundall, 2004). In this study, PFC software was employed for numerical simulations. Initially, the model's micro-parameters were calibrated using uniaxial, triaxial, and direct tensile tests on a synthetic rock made of cement and chalk. Subsequently, the direct shear test was simulated under constant normal stress. Conversely, a laboratorial DST has been done simultaneously with the acoustic emission analyses of cracks events. The result of these models have been verified with each other and utilized for investigation of effect of sample characteristics on the crack initiation and crack damage shear stress levels.

II. PHYSICAL MODELLING

For the both purposes of physical DST of intact rock with acoustic emission analyses and numerical modeling study a synthetic material made of 40% chalk, 20% percent Portland Cement (type II), and 40% water was used. In order to obtain the rock mechanical properties of this material, different tests, such as UCS, TCS and Brazilian test have been conducted on this material. Worth mentioning that in the preparation of the needed cylindrical sample for the above mention tests and cuboid sample for DST, all the samples were rested for 10 days. Based on the Asadizadeh et al. (2016) study for this type of material after 10 days of curing the variation of mechanical parameters are negligible.

Fig. 3 illustrates the mold used for producing samples and some of the conducted tests.

In Fig. 3, Size of the shown mold and sample which is under the UCS test is 125×53 mm and the unit weight of the sample is 1147.3 kg/m^3. The rock mechanical parameters of the rock sample are listed in Tables 1 and 2. With a different mold, a cuboid sample was made out of this synthetic material

a b c

Fig. 3. a) The mold used for sample creation b) Brazilian test c) UCS test.

Table 1. Result of USC and Brazilian tests on the synthetic rock sample

σ_c (MPa)	E (GPa)	ν	σ_t (MPa)
12.40	5.96	0.15	1.46

Note: σ_c:UCS, E: Young's Modulus, ν: Poisson's ratio, σ_t: Tension strength

Table 2. Result of TCS tests on the synthetic rock sample

Test Number	σ_3 (MPa)	σ_1 (MPa)
1	0	12.40
2	0.5	18.00
3	1	20.85
4	2	24.90
5	4	30.31

This cuboid sample was used for a DST test and at the same time acoustic emission (AE) analyses. Acoustic emission has become a widely used non-destructive technique in materials science. It utilizes transient elastic waves, generated by the rapid release of energy from localized stress points within a material. Unlike traditional methods that simply identify defects, AE testing provides real-time monitoring, offering valuable insights into the onset and progression of damage. This capability to detect micro-cracks and other stress-induced anomalies before they develop into major defects highlights the preventive maintenance benefits of the AE technique. Additionally, the method allows for continuous monitoring, ensuring that the structural health of critical components can be evaluated without interrupting their operation (Miller and McIntire, 1987). These mentioned benefits of AE analyses can help us to monitor the crack initiation and crack damage shear stresses during the DST in particular with the parameter called "cumulative hit". This parameter quantifies the total number of acoustic emissions recorded over a specific period or during a particular test, providing insights into the material's fracture processes. By analyzing cumulative hits, researchers can track the progression of damage, identify critical points of failure, and distinguish between different stages of material degradation. This approach provides a comprehensive understanding of the underlying mechanisms driving material failure (Moradian and Li, 2017).

A DST accompanied by AE analyses has been conducted on the rock sample of the introduced material. The DST has been done under the constant normal stress of 0.51 MPa with constant velocity following the ISRM suggested methods. In Fig. 4, the results of this laboratorial test is shown.

As shown in Fig. 4, peak shear strength occurred at 3.81 MPa. Moreover, it is tried to fit two linear lines (dashed lines) to the cumulative hits figures and it was observed that slope of this parameter graph has changed profoundly in two points which can be considered as crack initiation and crack damage stress respectively. In the physical modelling of DST on the rock sample of this study, crack initiation and crack damage stresses occurred in 67% and 91% peak shear strength, respectively. This result confirms previous studies (Alidaryan et al., 2023; Shang et al., 2021) in direct shear tests (DST) that these levels of stress occur much closer to the peak rather than compression stress conditions.

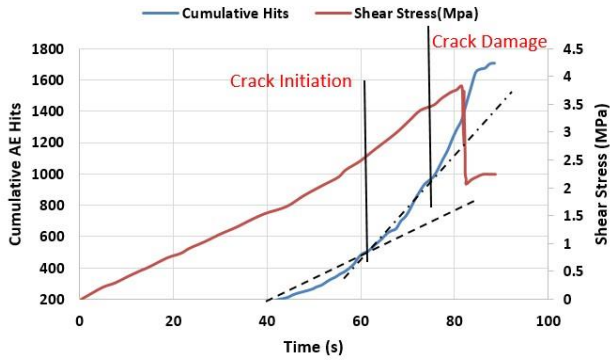

Fig. 4. Shear stress and cumulative hits vs. time graph of laboratory DST with AE analyses under σ_n of 0.51 MPa

III. NUMERICAL MODELLING

To investigate the mechanisms of crack initiation and propagation in intact rock under direct shear, numerical modeling using discrete elements and PFC2D software was also employed. In this software, the environment is simulated with rigid balls that can overlap at their contact points, representing the material's deformability. These balls can bond at contact points, acting like cement between particles. If the applied stress during the test exceeds the tensile or shear strength of these bonds, cracks form. The connection of these micro-cracks results in large-scale sample failure. This software thus allows for examining various rock properties, including crack initiation and propagation mechanisms.

It is important to note that laboratory parameters such as uniaxial compressive strength or tensile strength cannot be directly defined in the software. The parameters that can be defined include micro-properties like density, particle size, frictional properties, deformability of the balls, and the bonding properties between particles. Therefore, to simulate a rock sample, the contact bond model must first be chosen, and then through a calibration process, numerical test results like compressive tests are matched with physical test results. After recreating the desired rock sample in the numerical model, the desired test can be simulated and validated.

A. *Contact Model*

Three common bonding models for simulating particle interactions are the contact bond, parallel bond, and flat joint models. Potyondy (2018) used the flat joint model to simulate a type of intact rock, demonstrating that this model effectively represents rock behavior under various loading conditions. In another study, (Bahaaddini et al. 2021) evaluated different particle bonding methods and concluded that the flat joint model is more suitable for modeling the mechanical behavior of intact rock than other models. In this study, the flat joint model is utilized for simulating intact rock. Figure 5 shows how rock is simulated using the flat joint method. In this model, the contact points between two particles are divided into several smaller elements. These elements can either be bonded or unbonded. By defining the bonding ratio parameter, micro-cracks present in the sample can be simulated with a specific distribution.

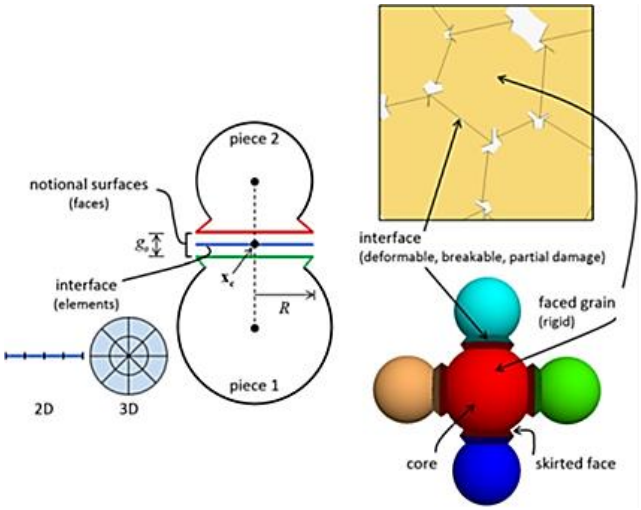

Fig. 5. Schematic illustration of Flat-Joint contact model (Potyondy, 2015)

B. *Calibration*

The calibration process aims to align the micro-scale mechanical properties of the numerically simulated sample with the experimentally obtained properties of the target sample. Essentially, the goal is to identify the micro parameters that, when used in the software, yield mechanical properties similar to those observed in laboratory tests. The Calibration in the PFC software is a time consuming trial-and-error process, however there are some guidelines to expedite it. The calibration process of this study follows the recommendations provided by Bahaaddini et al., 2021 and used by Mohsen Alidaryan et al., 2023 by simulating three tests: direct tensile, uniaxial compressive, and triaxial compressive. In Fig. 6, some of these simulated tests can be observed.

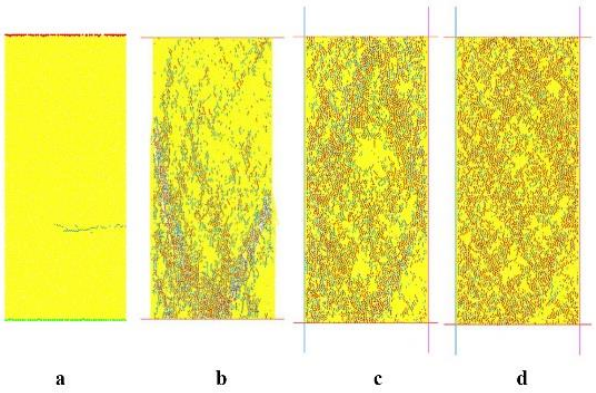

Fig. 6. Calibration process by simulation of mechanical tests: a) Direct Tension Test, b) UCS, C) TCS test with 0.5 MPa confining stress and d) TCS test with 4 MPa confining stress

The calibration steps, which involve an iterative process, can be outlined as follows: First, by simulating a direct tensile test and adjusting the micro parameters of the flat bond tensile strength and bonding ratio, the tensile strength reported in the laboratory test is aimed to be recovered. Next, by performing a uniaxial compressive test and modifying the normal-to-shear stiffness ratio of the bonds and particles, Poisson's ratio is recovered. In the third step, through an iterative process with the previous step, the elastic modulus is calibrated by altering the elastic modulus of the bonds and particles. Following this, the uniaxial compressive strength is recovered by changing the cohesion of the flat bonds. Finally, by conducting a triaxial compressive test under varying lateral stresses and modifying the flat bond friction angle and particle friction coefficient, the internal friction angle of the rock is calibrated. The calibrated numerical model parameters are presented in Table 3. Throughout the calibration process, the sample under investigation was simulated, and all these parameters were reproduced with an average error of 3.59%. The results related to the strength properties are compared with the laboratory results in Fig. 7. This study shows that the uniaxial, triaxial, and tensile test results for the calibrated sample have a satisfactory correlation with the laboratory results and calibration process was successful.

The result of Fig. 7 is also reviewed and illustrated in Table 4.

As it is shown in Table 4, all of the mechanical specification of the numerical model were successfully recovered by the average error of 3.26% relative to physical model. Therefore, by simulating DST using the crack monitoring tool in PFC software, it is now feasible to examine crack initiation and the shear stress associated with crack damage.

Table 3. Calibrated micro parameters of particles and the Flat-Joint contact model

Sample and particle parameters		Flat-joint contact model micro-properties	
Density (kg/m^3)	1147.3	Installation gap (mm)	0.04
R_{min} (mm)	0.4	Bonded fraction	0.98
R_{max} (mm)	0.6	Number of elements	2
Porosity	0.08	$\bar{E}_c$ (GPa)	6.45
Particle micro-properties		$\bar{k}_n/\bar{k}_s$	2.1
E_c (GPa)	6.45	Friction angle (°)	49.5
k_n/k_s	2.1	Cohesion (MPa)	7.15
Friction coefficient, μ	0.46	Tensile strength (MPa)	3.6
		Friction coefficient, $\bar{\mu}$	0.46

C. *DST Numerical Modelling*

To simulate the direct shear test, the dimensions of the shear boxes and the numerical sample under shear were chosen to match the laboratory dimensions. The micro-parameters calibrated for rock as listed in Table 3 were used to create the sample under shear. Creating the numerical sample within the shear box involved generating particles with a normal distribution and a specified range of radius (0.4–0.6 mm) at random positions, applying mechanical properties to the particles, and conducting computational cycles to move the particles and establish isotropic stress between them. Finally, flat-joint bond connections were installed for particles that are physically connected or within a certain distance from each other. A constant vertical stress of 0.51 MPa was applied to the sample via the top plate, and a self-control mechanism was used to maintain constant stress during the process.

Fig. 8 shows the simulated direct shear test and the final broken sample.

In Fig. 9, the graph of shear stress and number of cracks versus shear displacement of numerical model of DST shown.

Table 4. Comparison of mechanical parameters of physical against the numerical model

	σ_c (MPa)	σ_t (MPa)	E (GPa)	Nu	Mohr-Coulomb Parameters		Hoek-Brown Parameters	
					c (MPa)	ϕ (deg)	σ_{ci} (MPa)	m_i
Physical	12.4	1.46	5.96	0.15	2.905	42.61	14.3	9.693
Numerical	12.9	1.518	6.13	0.148	3.081	42.93	15.269	9.983
Error (%)	4.03	3.97	2.58	1.33	6.06	0.75	6.78	2.99

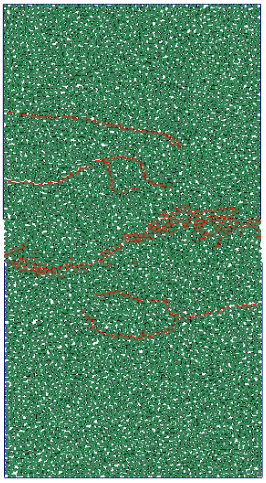

Fig. 7. Simulated DST with constant normal stress of 0.51 MPa (final broken sample with macro-cracks developed as red lines).

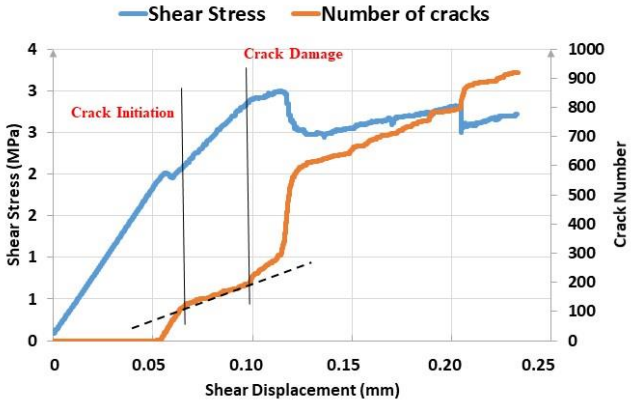

Fig. 8. Numerical simulation graph of DST on the synthetic rock sample under normal stress of 0.51 MPa.

As shown in Fig. 9, crack initiation and crack damage stresses occur in 69% and 94% percent of peak shear strength. Notice that based on the definition of crack initiation which is an indicator of stable crack growth, the rapid temporary growth in crack numbers just after 0.05 mm displacement, cannot be attributed to this shear stress level. An accidental micro failure happened in upper body of sample in laboratory and does not related to the main failure plane. This phenomenon is natural in physical experiments and does not affect the whole result. The average error of result of numerical simulation concerning the physical models is 3% which means that the numerical modeling is valid and confirms previous findings in DSTs that these levels of stresses occur much closer to the peak rather than compression stress conditions.

IV. Result and Discussion

As mentioned in the Introduction of this paper, the effective parameters on the crack initiation and crack damage stress levels in compression tests are mostly related to rock characteristics such as porosity, tensile strength, grain size, veins, and etc. However, the investigation about these stress levels are limited in shear stress conditions.

The result of previous studies and present investigation on DSTs crack initiation and crack damage stress levels are briefly reviewed in Table 5.

As shown in the Table 5, the result of both numerical and physical models of present study confirm previous findings that crack initiation and crack damage shear stress levels occur closer to the peak rather than the compression tests. Moreover, the three compared materials in the table 5, granite, sulfaset and the rock sample of present study, have different specifications in grain size, strength, etc. For example, the peak shear strength of granite sample in Shang et al. (2021) study is about 6 times that of rock sample of present study. Also, the chalk and cement grain sizes are too small against the granite. Therefore, it can be concluded that rock characteristics affect the crack initiation and crack damage shear stress as same as compression stress condition.

Table 5 Overview of previous studies and present investigation on DSTs crack initiation and crack damage stress levels

Row	Material	Type of study	Crack Initiation shear stress %	Crack Damage shear stress %
1	Granite (Shang et al., 2021)	Physical	80	88
2	Sulfaset (Alidaryan et al., 2023)	Numerical	91	95
3	Chalk and Cement (Present Study)	Physical	67	91
4	Chalk and Cement (Present Study)	Numerical	69	94

V. Conclusion

This study utilizes physical modeling combined with acoustic emission analysis and numerical modeling using the discrete element method (PFC software) to investigate crack initiation and damage stresses in direct shear tests. Initially, the properties of the numerical model were calibrated using tensile, uniaxial compressive, and triaxial tests. Subsequently, a direct shear test was simulated, and the numerical results were compared with laboratory results to validate the numerical model. The result showed that there is a good agreement between these two models. This research confirms previous findings that shear crack initiation and damage stresses occur closer to peak strength than compressive tests. For instance, these stress levels occurs in UCS around 40 and 75 percent of peak stress in the study of Martin and Chandler (1994), while these figures for DST are around 67 and 91 in this study. It is also demonstrated that crack initiation and damage stresses in shear tests depend on the characteristics of

the tested rock, similar to compressive tests. As these stress levels are important in instability problems in underground projects or other infrastructures including rock materials, the findings of this study can be used for investigation of failures in shear mode and help to preventing of that in mentioned projects. Moreover, for further study, it is recommended to use multiple samples with varying porosities and grain sizes to more accurately investigate the direct or indirect relationship of these effects.

REFERENCES

Alidaryan, M, Khosravi, M. H., Bahaaddini, M., Moosavi, M., & Roshan, H. (2023). Mobilization of Cohesion and Friction Angle of Intact Rocks in the Shearing Process. Rock Mechanics and Rock Engineering, 56(11), 8221–8233.

Alidaryan, Mohsen, Khosravi, M. H., Bahaaddini, M., & Moosavi, M. (2023). Investigation of crack initiation and crack damage stresses in intact rock shear failure. Journal of Mining Engineering, 18(60), 46–55.

Amann, F., Ündül, Ö., & Kaiser, P. K. (2014). Crack initiation and crack propagation in heterogeneous sulfate-rich clay rocks. Rock Mechanics and Rock Engineering, 47, 1849–1865.

Asadizadeh, M., Hossaini, M. F., Moosavi, M., & Mohammadi, S. (2016). A laboratory study on mix design to properly resemble a jointed brittle rock. A Laboratory Study on Mix Design to Properly Resemble a Jointed Brittle Rock, 50(2), 201–210. https://doi.org/10.22059/ijmge.2016.59830

Bahaaddini, M., Sheikhpourkhani, A. M., & Mansouri, H. (2021). Flat-joint model to reproduce the mechanical behaviour of intact rocks. European Journal of Environmental and Civil Engineering, 25(8), 1427–1448. https://doi.org/10.1080/19648189.2019.1579759

Bello Garcés, S. (2018). Ideas previas y cambio conceptual. In Educación Química (Vol. 15, Issue 3). https://doi.org/10.22201/fq.18708404e.2004.3.66178

Bieniawski, Z. T. (1967). Mechanism of brittle fracture of rock: part I—theory of the fracture process. International Journal of Rock Mechanics and Mining Sciences & Geomechanics Abstracts, 4(4), 395–406.

Eberhardt, E., Stead, D., Stimpson, B., & Read, R. S. (1998). Identifying crack initiation and propagation thresholds in brittle rock. Canadian Geotechnical Journal, 35(2), 222–233.

Lajtai, E. Z., & Lajtai, V. N. (1974). The evolution of brittle fracture in rocks. Journal of the Geological Society, 130(1), 1–16.

Li, C., Xie, H., & Wang, J. (2020). Anisotropic characteristics of crack initiation and crack damage thresholds for shale. International Journal of Rock Mechanics and Mining Sciences, 126, 104178.

Martin, C. D., & Chandler, N. A. (1994). The progressive fracture of Lac du Bonnet granite. International Journal of Rock Mechanics and Mining Sciences And, 31(6), 643–659. https://doi.org/10.1016/0148-9062(94)90005-1

Miller, R. K., & McIntire, P. (1987). Nondestructive testing handbook. vol. 5: Acoustic emission testing. American Society for Nondestructive Testing, 1987, 603.

Moradian, Z., & Li, B. Q. (2017). Hit-based acoustic emission monitoring of rock fractures: Challenges and solutions. Advances in Acoustic Emission Technology: Proceedings of the World Conference on Acoustic Emission–2015, 357–370.

Mutaz, E., Serati, M., Bahaaddini, M., & Williams, D. J. (2021). On the evaluation of crack initiation stress threshold. ARMA US Rock Mechanics/Geomechanics Symposium, ARMA-2021.

Ning, J., Wang, J., Jiang, J., Hu, S., Jiang, L., & Liu, X. (2018). Estimation of crack initiation and propagation thresholds of confined brittle coal specimens based on energy dissipation theory. Rock Mechanics and Rock Engineering, 51, 119–134.

Peng, J., Rong, G., & Jiang, M. (2018). Variability of crack initiation and crack damage for various rock types. Arabian Journal of Geosciences, 11, 1–10.

Potyondy, D O. (2018). A flat-jointed bonded-particle model for rock. 52nd US Rock Mechanics/Geomechanics Symposium.

Potyondy, David O., & Cundall, P. A. (2004). A bonded-particle model for rock. International Journal of Rock Mechanics and Mining Sciences, 41(8 SPEC.ISS.), 1329–1364. https://doi.org/10.1016/j.ijrmms.2004.09.011

Potyondy, David Oskar. (2015). The bonded-particle model as a tool for rock mechanics research and application: current trends and future directions. Geosystem Engineering, 18(1), 1–28.

Rafiei Renani, H., & Martin, C. D. (2018). Cohesion degradation and friction mobilization in brittle failure of rocks. International Journal of Rock Mechanics and Mining Sciences, 106(March), 1–13. https://doi.org/10.1016/j.ijrmms.2018.04.003

Rahjoo, M. (2019). Directional and 3-D confinement-dependent fracturing, strength and dilation mobilization in brittle rocks. University of British Columbia.

Shang, D., Chen, Y., Zhao, Z., Shangguan, S., & Qi, X. (2021). Mechanical behavior and acoustic emission characteristics of intact granite undergoing direct shear. Engineering Fracture Mechanics, 245, 107581. https://doi.org/10.1016/j.engfracmech.2021.107581

Zhang, G. K., Li, H. B., Wang, M. Y., & Li, X. F. (2020). Crack initiation of granite under uniaxial compression tests: A comparison study. Journal of Rock Mechanics and Geotechnical Engineering, 12(3), 656–666.